The Effect of TiO2 Film Immersion Duration in N719 Dye on Microstructure, Optical Properties, and Photoanode Performance of Photosupercapacitors Based FTO/TiO2/N719/Activated Carbon/Carbon Black

Markus Diantoro[1,2,3(✉)], Ida Vaeruza Albadi'ah[1], and Nasikhudin[1]

[1] Department of Physics, Faculty of Mathematics and Natural Sciences,
Universitas Negeri Malang, Jl. Semarang 5, Malang, Indonesia
`markus.diantoro.fmipa@um.ac.id`

[2] Center of Advanced Materials for Renewable Energi, CAMRY, Universitas Negeri Malang,
Jl. Semarang 5, Malang, Indonesia

[3] Center of Supercapacitors and Energy Storage, CSES, Universitas Negeri Malang,
Jl. Semarang 5, Malang, Indonesia

Abstract. Photosupercapacitor (PSC) is integrated harvesting (DSSC) and storing energy (supercapacitor) simultaneously. The increase in DSSC performance is studied through an effect of TiO2 film immersion duration on the N719 dye, which has not been investigated so far. Furthermore, the effect of stacking configuration on the performance of FSC was investigated. There are three steps of fabrication; the first is DSSC fabrication, the second is supercapacitor fabrication, and the last is the integration of both devices as FSC. The DSSC was fabricated by depositing TiO2 paste from solaronix and then immersed into a dye solution with 7, 12, 17, 22, and 27 h immersion duration.

Meanwhile, the supercapacitor was fabricated by mixing AC, CB, and SBR for 24 h, then deposited on the Al foil substrate and followed by the heating process. The next step is to integrate both devices as FSC in series and parallel configurations. XRD, UV-Vis, EIS, and I-V characterized the DSSC. Besides, the supercapacitor performance was characterized by CD, and the FSC performance was assessed through photoresponse. The results showed that the increase in immersion time was proportional to the absorbance and efficiency of DSSC. The increase in the absorbance caused more Dye to be absorbed in the TiO2 pores, which affects the photon capacity that contributes to the DSSC performance. DSSC efficiency reaches saturation at 22h immersion time with 4,39% efficiency. The specific capacitance of the supercapacitor is 61.35 F/g. The discharge time on the FSC is shown exponential following the discharge characteristics of the supercapacitor.

Keywords: Photosupercapacitor (PSC) · DSSC · supercapacitor · immersion time · dye N719

1 Introduction

A solar cell is an electronic device that directly converts solar energy into electrical energy through the photovoltaic mechanism. DSSC is the third generation of solar cells. DSSC was more attractive than the previous generation due to its simpler fabrication, processing at room temperature, low fabrication cost, and being made from organic materials, so it minimizes environmental impact [1]. Photoanode is one of the most important parts of DSSC because, in this section, electron recombination occurs [2]. Many factors affect the performance of photoanodes, such as morphology, thickness, and Dye [3]. As a sensitizer, Dye plays a key role in absorbing photons from sunlight and converting them into electric current.

Research to optimize the immersion duration of photoanode on the Dye N719 has been carried out widely. A study on the effect of immersion time on the ZnO-based DSSC efficiency reported that the efficiency increased from 0.38% to 0.44% with the increase in immersion duration [4]. A similar study found that the efficiency of ZnO/N719-based DSSC was reported to increase up to 0.62% at increasing immersion time from 1 to 2 h [5]. The studies on the effect of TiO2 film immersion duration on Dye N719 have been carried out using a short time ranging from 5 min to 8 h; then, the test is jumped at 24 h. In that study, phenomena between 8 to 24 h were not observed.

Furthermore, the characterization only covers the absorbance and efficiency of DSSC, so the phenomena that occur on the effect of increasing the immersion duration cannot be explained in detail [6]. In addition, the reported performance is still quite low due to the unoptimum synthesis factor. One way to improve DSSC performance is through photoanode modification using commercial TiO2 paste from Solaronix.

TiO2-based DSSC utilizing commercial paste from Solaronix had achieved an efficiency of 3.70% [7]. Another study using commercial TiO2 paste from solaronix obtained a light conversion efficiency of 3.65% [8]. Therefore, this study was conducted on the effect of immersion time of TiO2 film on Dye N719 with 7, 12, 17, 22, and 27 h of various duration. The characterization was carried out on microstructure, optical properties, energy conversion efficiency, Voc, and electrons lifetime to explain the phenomena in more detail.

The photoanode film used was based on commercial TiO2 paste from Solaronix, which resulted in high efficiency. This research is important because the immersion time of TiO2 film on Dye N719 is directly related to the amount of Dye that can be adsorbed, so it affects the efficiency of DSSC.

The other side that can be developed is the integration of DSSC with energy storage devices to maintain the stability of energy availability [9]. Integrating DSSC with a supercapacitor is known as a photo supercapacitor (PSC). This device was a simpler, lighter, cheaper, and self-charging system [10].

2 Method

2.1 Dye-Sensitized Solar Cell Fabrication

DSSC is fabricated by using commercial materials. Fluorine-doped tin oxide (FTO), blocking layer (BL-1), and mesoporous TiO2 (18-NR-T Titania paste) were purchased from Greatcell, China. Reflective layer (TI-Nanoxide R/SP), N719 dye (Ruthenizer), Pt

drill, Surlyn 25 µm (SX1170–25, Solaronix), and the redox electrolyte (mostly TDE 250) were obtained from Solaronix S.A., Aubonne, Switzerland.

The first step was clean up FTO with an ultrasonic bath. FTO sink on the detergent and DI water for 15 min, then immerse in the warm ethanol and dry it. The Clean FTO was ready to be coated by a blocking layer. They were blocking layers deposited on the FTO substrate using spin coating at 3000 rpm for 30 s. Let it be at room temperature for about 5 min and then heated at 100, 300, and 500 °C. The next step was to deposit mesoporous TiO2 (18 NR-T Titania paste) in an active surface area of 1.0 cm x 1.0 cm by a screen printing method. The next layer which has deposited was the reflective layer. The deposition of the reflective layer (Ti-Nanoxide R/SP, Solaronix) used a screen printing technique with T-60 mesh. The film was heated at 100, 300, and 500 °C for 15, 15, and 30 min for every layer, respectively. The next step is to prepare for post-treatment by stirring a solution of 20 mL 2-propanol and 150 µL Titanium (IV) (triethanolamine) isopropoxide (TTEAIP) for 15 min. This film was then immersed in the post-treatment solution and heated at 75 °C for 30 min in the microwave. Afterward, these films were immersed in the solution of N719 (Solaronix S.A., Switzerland) for 7, 12, 17, 22, and 27 h in dark conditions. After preparing this electrode, the assembled electrode with Pt was drilled into a sandwich structure. 25µm-thick Surlyn separated the sandwich electrode structure. The last step is to inject Ionic Liquid Electrolyte (Mosalyte TDE 250, Solaronix) into those assembled cells.

2.2 Synthesis Carbon-Based Electrode of Supercapacitors

Supercapacitor production's first step is the synthesis of carbon paste. The synthesis of carbon paste was started by mixing SBR binder solution and DI water until homogeneous. After that, AC and CB powder is added and stirred at 300 rpm. After vigorously stirring for 24 h with a magnetic stirrer, the carbon paste was ready to deposit on an aluminum foil sheet. The aluminum foil sheet was chosen as the substrate due to its low cost, flexibility, and considerable conductivity. The aluminum foil substrate was coated by homogeneous and viscous carbon paste using the doctor blade technique with 100 µm thickness. The process continued to dry the film in the microwave at 80 °C for 1 h. Then two electrodes were face-to-face assembled with a piece of the separator as the membrane. The assembled package was then filled with an electrolyte ET4NBF4 1M.

2.3 Assembly of Photo-Supercapacitor

The PSC has a multi-layer structure, including a photoactive electrode and Pt drill glass of DSSC at the upper side and the compact inner layer, compact outer layer, and a diffuse layer of supercapacitors on the bottom side. The device structure is shown in Fig. 1.

2.4 Characterization and Measurement

The X-ray diffraction pattern of TiO2 photoanode was obtained from XRD PAN analytical XPER-3 with radiation from a Cu target (Kα wavelength = 1.540598 Å). The position of 2-theta is in the range of 20–90°. Photo current-voltage measurements of
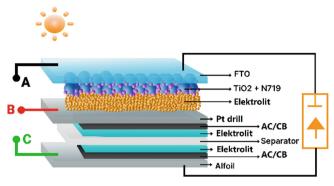
Fig. 1. Schematic of photo-supercapacitor

DSSC are done under simulated solar illumination (100 mW/cm^2) and measured by PECL IV-meter Keithley 6517B—the electrochemical performance of supercapacitor, cycling performance, and galvanostatic charge-discharge measurement using Netware Battery Tester. The integrated photo supercapacitor's performance was measured under illuminating solar simulator and IV-meter Keithley 2400 to obtain photo-voltage.

3   Results and Discussion

The crystallographic analysis of the samples was carried out by a PAN analytical XPER-3 X-ray diffractometer (XRD). Figure 2 (a) shows the XRD spectrum of the DSSC film. The cell comprises a blocking, mesoporous TiO2, and a reflective layer. All of the witnessed peaks in the spectrum are attributed to the TiO2 tetragonal crystal system, which corresponds to the anatase phase of the COD database of 2310710. As shown in the figure, there are no impurity phases or other oxides in the crystal structure.

XRD pattern of TiO_2 anatase was analyzed by refinement using Software GSAS with the matching process with the COD database of 2310710 in space group I 41/an m d lattice parameter a = b = 3.8720, c = 9.6160, α = β = γ = 90°. All the Bragg peaks in the XRD pattern can be indexed well to the anatase TiO2 phase COD 2310710. The structure of TiO2 anatase show peaks at point and indexed to; 25.3° (011), 37.9° (013), 37.8° (004), 30.7° (112), 48.1° (020), 53.9° (105), 55.2° (121), 62.6° (024), 68.8° (211), and 75.1° (125). Results of refinement lattice parameter a = b = 3.781, c = 9.501, α = β = γ = 90° which indicate the tetragonal crystal system. The reliability Rietveld refinement are Rp = 0.2172, Rwp = 0.3032, dan χ2 = 1.66.

The diffraction pattern of TiO2 with 7, 12, 17, 22, and 27 h of immersion duration is shown in Fig. 4.4. The diffraction pattern showed that the TiO2 diffraction peak was observed at the same 2θ angle, but the peak height differed for each immersion time variation. The crystallinity of the diffraction pattern was analyzed, and the calculation shows that the crystallinity tends to decrease with increasing immersion time. The crystallinity at immersion times 7, 12, 17, 22, and 27 was 34.92; 38.71; 31.67; 29, 64, and 28.59%. Similar results were obtained in a previous study that reviewed the effect of immersion time of TiO2 photoanode in 0.5 mM dye N719 solution, which resulted in a crystallinity decrease with a longer immersion time [11].
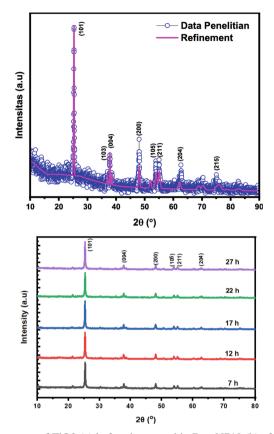
Fig. 2. Diffraction pattern of TiO2 (a) before immersed in Dye N719 (b) after immersed in Dye N719

The UV-Vis spectra of samples without dye immersion (0 h immersion) showed one absorption peak at 340 nm. In contrast, samples with 7, 12, 17, 22, and 27 h immersion times showed two absorption peaks at 340 nm and 520 nm, representing the N719 absorption. The graph of the UV-Vis was analyzed by calculating the area under the curve, which shows the film absorbance [12] (Fig. 3).

The absorbance of TiO2 photoanode film at 0, 7, 12, 17, 22, and 27 h immersion time was 762.00; 924.12; 878, 01; 975.54; 1005.16 and 1009.51 a.u. These results indicate that the increase in immersion duration is proportional to the absorbance. It is shown that the increase in immersion duration would increase the number of dye molecules attached to the TiO2 film. Similar results have been reported that increasing the immersion time increased the absorbance of the photoanode film [13]. The film owned the highest absorbance of 1009.51 a.u with an immersion time of 27 h. According to Chang et al., the adsorption time of the Dye must be long enough so that the interface surface of the oxide film is completely covered by a single layer of dye molecules [14].

The energy gap of TiO2 was obtained by plotting the absorption data using the direct transition equation. The band gap value is calculated by extrapolating the linear part of
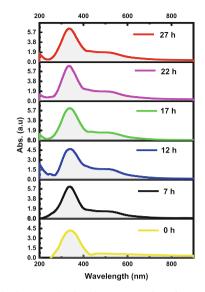
Fig. 3. TiO2 photoanode absorbance at various immersion duration

the curve to the absorption line. The graph of the relations $(\alpha h\upsilon)$ 2 vs. eV is shown in Fig. 4(a), while the relation between the immersion time and the energy gap at the TiO2 /N719 photoanode is shown in Fig. 4(b).

The results show that there are two energy gaps, where the energy gap in the range of 3.22 - 3.31 eV represents the energy gap of TiO2, and the energy gap in the range of 1.95 - 2.02 eV represents the Dye N719. The sample with 0 h only shows one Eg, which is 3.31 eV; the sample is not immersed in N719, so there is no absorption of N719 on the TiO2 film. The results of the linear fitting show that both energy gaps decreased with increasing dye immersion time. A film with a dye immersion time of 7, 12, 17, 22, and 27 h showed a decrease in the energy gap of TiO2, respectively 3.26; 3.23; 3.24; 3.23, and 3.21 eV. Meanwhile, the energy gap on the N719 also decreased by 2.01, respectively; 1.98; 1.97; 1.96, and 21.95 eV with dye immersion times of 7, 12, 17, 22, and 27 h. The decrease in gap energy is induced by charge transfer due to the addition of immersion time which causes a change in the charge density in the TiO2 semiconductor. The change in charge density indicates a rearrangement of the electronic structure of the Dye and the semiconductor as a consequence of their surface interactions. These results are in accordance with previous studies which showed the effect of immersion time on N719 on the shift of the semiconductor conduction band and dye conduction band [5, 15]. Previous studies showed the energy gap decreased from 3.3 to 3.1 eV after 26 h of immersion [16]. The decrease in the energy gap in TiO2 allows the injection of dye electrons from the valence band to the conduction band of TiO2 to be easier because it requires lower photon energy for the electron excitation mechanism.

DSSC performance is obtained by measuring the electrical properties expressed as a J-V curve. Measurements were carried out by irradiating using light with an intensity of 100 W/m2. In this irradiation, the condition will occur excitation of electrons, which
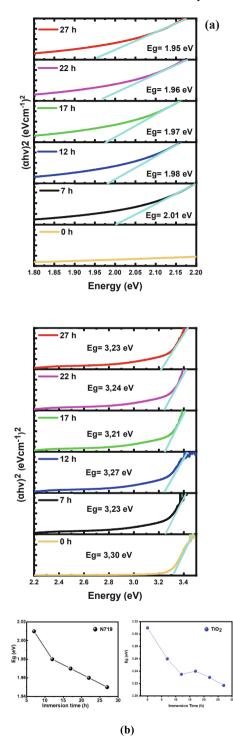
(a)

(b)

Fig. 4. (a) (αhυ)2 vs. eV with linear fittings at 340 nm and 380 nm (b) immersion time Vs. Energy gap TiO2/N719 photoanode with an immersion time of 0.7,12,17,22 and 27 h

causes a current. The active area of the DSSC used is 1 cm2. Figure 5 shows the results of the J-V characterization of DSSC with variations in immersion time on TiO2 films.

The efficiency of DSSC increased with increasing immersion time. The increase in efficiency reached the saturation point at an immersion time of 22 h. Thus, the efficiency decreased for a longer immersion time of 27 h. This is because the more the immersion time increases, the more dye sticks to the TiO2 film layer. The higher amount of Dye was proportional to the photon energy, thus increasing the chance of electron excitation. This number of excited electrons causes more electrons to go to the counter electrode, thereby increasing the Jsc generated in the conversion process and resulting in higher DSSC efficiency [17]. The decrease in efficiency occurred at an immersion time of 27 h, even though the amount of Dye absorbed increased. This is because the dye molecules cannot transfer the photogenerated electrons to TiO2. After all, they tend to aggregate [18].

The relation between immersion time and DSSC efficiency and comparison with reference data is shown in Fig. 6 [19]. Previous research on TiO2 photoanode films synthesized from TiO2, PEG6000, and Ethanol powder with 9 μm film thickness showed similar results where the efficiency of DSSC increased with increasing immersion time and decreased after passing saturation time. The saturation time achieved in that study was 8 h; the result showed a decrease in efficiency due to dye molecules aggregating on the surface of the semiconductor after 24 h, thereby inhibiting charge transfer and worsening the performance of DSSC [19].
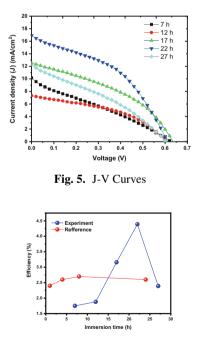

Fig. 5. J-V Curves

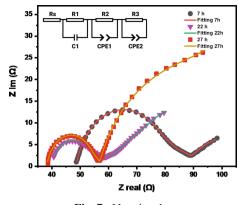**Fig. 6.** Effect of immersion time on DSSC efficiency Vs reference

Fig. 7. Nyquist plot

EIS characterization is recommended to investigate the electron transport kinetics and recombination in DSSC [20]. EIS characterization was carried out using Gamry 3000 reference tool, using a frequency range of $0.1–1 \times 105$ Hz, amplitude modulation of AC voltage of 10 mV, and DC bias voltage of 0 - 0.6 V. Determination of the resistance value on the EIS curve was carried out through fittings using the equivalent circuit. The results of the Nyquist plot fitting on the effect of immersion time on the performance of the DSSC film are shown in Fig. 7, and the equivalent circuit is modeled as shown in the inset of the figure.

The resistance parameter Rs obtained from the Nyquist plot on samples with immersion times of 7, 22, and 27 h was 48.46, 38.61, and 38.35 Ω while the parameter R2 (Rct) in samples with an immersion time of 7, 22, and 27 h, respectively 33.53, 16.52, and 15.27 Ω. Changes in Rs and Rct can be related to changes in the number of dye molecules on the photoanode, which contributes greatly to the internal impedance. The internal impedance of the samples 7, 22, and 27 h, respectively, is 52.01, 40.02, and 57.02. The decrease in resistance with increasing immersion time occurs due to electron traps which causes the DSSC resistive element to decrease. Previous reports also mentioned that the resistive element of DSSC decreases with an increasing number of adsorbed dye molecules [21, 22]. High resistance represents poor photovoltaic characteristics due to the much higher probability of recombination of electron-hole pairs in the diffusion process [23]. Photoresponse measurements were carried out with 100 mW/cm2 irradiation. Photoresponse of DSSC with variations in immersion time of 7, 12, 17, 22, and 27 h, and the measurement scheme is shown in Fig. 8. Measurements were made by irradiating for 20 s and then stopping the irradiation for 20 s. This result could determine the response of the sample that produces a voltage when given irradiation, while in dark conditions, the sample does not produce a voltage.

The DSSC photoresponse curve shows the maximum Voltage for 7, 12, 17, 22, and 27 h respectively, is 0.38; 0.30; 0.41; 0.56, and 0.35. The data trend follows the results of absorbance, crystallinity, impedance, and I-V tests where samples 7, 17, and 22 h have increased while samples for 27 h have decreased. The 12-h sample experienced a drastic decrease in Voltage due to 12-h sample damage. The addition of immersion time has
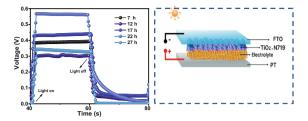
Fig. 8. DSSC photoresponse curves at various immersion times and their measurement schemes

increased the amount of Dye adsorbed on the TiO2 surface so that the electron mobility produced in the photovoltaic process is higher so that the measured Voltage is higher.

The increase in immersion time also decreases recombination at the TiO2/electrolyte interface, which can be measured directly from the cell's open-circuit voltage decay (OCVD). The motion of electrons at the interface of the semiconductor with the electrolyte is determined by the slope of the electron decay rate on the OCVD graph, as shown in Fig. 4.13. In the OCVD test, the lifetime of electrons is determined by the following equation.

$$\tau_d = -\frac{k_b T}{e}\left(\frac{dv}{d}\right)^{-1} \tag{1}$$

where kb is the Boltzmann constant, T is the temperature, e is the electron charge, and Voc is the open-circuit Voltage. The electron lifetime (τd) is related to the recombination process [2].

From Fig. 9, it is known that a sharp slope indicates a fast voltage decay and indicates a short electron lifetime. Previous studies have stated that OCVD is influenced by modification of the DSSC material, which is associated with an increase in electron lifetime [24]. To clarify the discussion of the effect of immersion time on efficiency, Voc, and lifetime, as well as supporting data on absorbance and crystallinity analysis, a graph of the relationship of all variables is shown in Fig. 10.

The increase in immersion time has increased the efficiency of DSSC in the range of 7, 12, 17, and 22 h and decreased at 27 h due to dye aggregation, which blocks electron excitation. The resulting trend is the same as the test results for the absorbance, lifetime, and Voc parameters and inversely proportional to the crystallinity parameter. In the 12-h
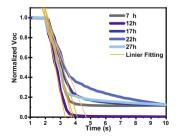

Fig. 9. OCVD curve on DSSC with the variation of immersion time
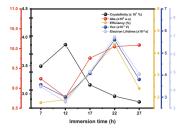
Fig. 10. Relation between efficiency, crystallinity, absorbance, electron lifetime, and Voc at various immersion times

sample, the increase was very low, only 6.91%, while the increase in other variations was 28.01%. This low increase indicates damage to the 12-h sample. This indication is supported by the test results on the absorbance, lifetime, and Voc parameters which decrease in the 12-h sample.

DSSC and supercapacitors successfully fabricated are then integrated into PSC devices. The DSSC sample used in this integration is a 22-h sample which produces the best efficiency, while the supercapacitor used is AC/CB-based electrode. Photoresponse measurement in the DSSC section is carried out to determine the ability of the DSSC to generate Voltage in the integrated device. Measurements were carried out by providing 100 mW/cm2 irradiation on the DSSC and then measuring the Voltage at terminals A and B. The results of photoresponse measurements and their measurement schemes are shown in Fig. 11.

The charging process is carried out by connecting terminals A and C to connect the PSC in a closed circuit. Simultaneously, irradiation with an intensity of 100 mW/cm2 was performed on the DSSC device. The voltage response across the supercapacitor area at terminals B and C is measured to assess the energy storage capability. In the irradiation condition, the charging process occurs; on that condition, the dye N719 is photoexcited, then the excited electrons are collected by the counter electrode through the TiO2 conduction band for further transfer to the supercapacitor section so that the FSC will work to harvest energy while storing it in the supercapacitor device. At the same time, the discharging condition is achieved by stopping the irradiation so that the charging current is cut off and causes the discharge to occur.
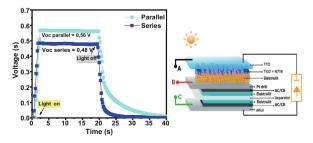

Fig. 11. Photoresponse PSC

4   Conclusion

Increasing the immersion time of TiO2 film on Dye N719 has caused a decrease in crystallinity and an increase in photoanode absorbance increase in efficiency. The increase in efficiency reaches saturation at 22 h with an efficiency of 4.39%. Efficiency decreased at 27 h of immersion due to the aggregation of dye molecules. The increasing immersion time of TiO2 was affected by the increase of Voc and electron lifetime. The measured Voc is 0.56 V, while the maximum lifetime is 0.069 s, achieved at an immersion time of 22 h. The decrease in Voc occurred in the 27-h sample because too many dye molecules were adsorbed, which inhibited the electron flow in the TiO2. Semiconductor The PSC was already fabricated using 22 h immersion duration DSSC and AC/CB-based supercapacitor. The result shows an exponential graph, which indicates an energy storage function.

References

1. Gong, Jiawei, K. Sumathy, Qiquan Qiao, dan Zhengping Zhou. 2017. "Review on dye-sensitized solar cells (DSSCs): Advanced techniques and research trends." Renewable and Sustainable Energy Reviews 68 (July 2016): 234–46. https://doi.org/10.1016/j.rser.2016.09.097.
2. Saeidi, Mahsa, Masoud Abrari, dan Morteza Ahmadi. 2019. "Fabrication of dye-sensitized solar cell based on mixed tin and zinc oxide nanoparticles." Applied Physics A: Materials Science and Processing 125 (6): 1–9. https://doi.org/10.1007/s00339-019-2697-3.
3. Umale, Sanjivani V., Sneha N. Tambat, Vediappan Sudhakar, Sharad M. Sontakke, dan Kothandam Krishnamoorthy. 2017. "Fabrication, characterization and comparison of DSSC using anatase TiO2 synthesized by various methods." Advanced Powder Technology 28 (11): 2859–64. https://doi.org/10.1016/j.apt.2017.08.012.
4. Singh, Amrik, Devendra Mohan, Dharamvir S. Ahlawat, dan Richa. 2016. "Influence of dye loading time and electrolytes constituents ratio on the performance of spin coated zno photoanode based dye sensitized solar cells." Oriental Journal of Chemistry 32 (2): 1049–54. https://doi.org/10.13005/ojc/320229.
5. Aksoy, Seval, Kamuran Gorgun, Yasemin Caglar, dan Mujdat Caglar. 2019. "Effect of loading and standbye time of the organic dye N719 on the photovoltaic performance of ZnO based DSSC." Journal of Molecular Structure 1189: 181–86. https://doi.org/10.1016/j.molstruc.2019.04.040.
6. Anggraini, R., F. Nurosyid, dan T. Kusumaningsih. 2020. "Dye sensitized solar cell (DSSC) with immersion time variation of working electrode on the dye of C4 plant chlorophyll of corn leaves (Zea mays L.)." AIP Conference Proceedings 2217. https://doi.org/10.1063/5.0000600.
7. Zhang, Xi, Xuezhen Huang, Chensha Li, dan Hongrui Jiang. 2013. "Dye-sensitized solar cell with energy storage function through PVDF/ZnO nanocomposite counter electrode." Advanced Materials 25 (30): 4093–96. https://doi.org/10.1002/adma.201301088.

8. Aprilia, Annisa, Waode Sukmawati Arsyad, R.N. Lamuda, Fitrilawati Fitrilawati, Norman Syakir, dan Rahmat Hidayat. 2016. "Kopolimer Hibrid Tmspma:Tems Sebagai Matriks Ionik Pada Sel Surya Tersensitisasi Dye." Spektra: Jurnal Fisika dan Aplikasinya 1 (2): 195–200. https://doi.org/10.21009/spektra.012.15.

9. Pierre, Balthazar, Raphael Clerc, dan Ana Claudia. 2017. "Solar Energy Materials and Solar Cells Theoretical analysis and characterization of the energy conversion and storage e ffi ciency of photo-supercapacitors." Solar Energy Materials and Solar Cells 172 (July): 202–12. https://doi.org/10.1016/j.solmat.2017.07.034.

10. Wee, Grace, Teddy Salim, Yeng Ming Lam, Subodh G. Mhaisalkar, dan Madhavi Srinivasan. 2011. "Printable photo-supercapacitor using single-walled carbon nanotubes." Energy and Environmental Science 4 (2): 413–16. https://doi.org/10.1039/c0ee00296h.

11. Sadikin, S. N., M. Y.A. Rahman, dan A. A. Umar. 2019. "Zinc sulphide-coated titanium dioxide films as photoanode for dye-sensitized solar cells: Effect of immersion time on its performance." Superlattices and Microstructures 130 (3): 153–59. https://doi.org/10.1016/j.spmi.2019.04.026.

12. Rahman, M. Y.A., L. Roza, S. A.M. Samsuri, dan A. A. Umar. 2018. "Effect of N719 Dye Dipping Temperature on the Performance of Dye-Sensitized Solar Cell." Russian Journal of Electrochemistry 54 (10): 755–59. https://doi.org/10.1134/S1023193518100051.

13. Jagtap, Chaitali V., Vishal S. Kadam, Mahadeo A. Mahadik, Jum Suk Jang, Nandu B. Chaure, dan Habib M. Pathan. 2022. "Effect of Binder Concentration and Dye Loading Time on Titania Based Photoanode in Dye Sensitized Solar Cell Application." Engineered Science 17: 133–41. https://doi.org/10.30919/es8d581.

14. Chang, Wei Chen, Chia Hua Lee, Wan Chin Yu, dan Chun Min Lin. 2012. "Optimization of dye adsorption time and film thickness for efficient ZnO dye-sensitized solar cells with high at-rest stability." Nanoscale Research Letters 7 (1): 1–10. https://doi.org/10.1186/1556-276X-7-688.

15. Ronca, Enrico, Mariachiara Pastore, Leonardo Belpassi, Francesco Tarantelli, dan Filippo De Angelis. 2013. "Influence of the dye molecular structure on the TiO2 conduction band in dye-sensitized solar cells: Disentangling charge transfer and electrostatic effects." Energy and Environmental Science 6 (1): 183–93. https://doi.org/10.1039/c2ee23170k.

16. Krisdiyanto, Didik, Siti Khuzaifah, Khamidinal Khamidinal, dan Enduraji Sedyadi. 2015. "Influence of Dye Adsorbtion Time on TiO2 Dye-Sensitized Solar Cell with Krokot Extract (Portulaca Oleracea. L) as A Natural Sensitizer." The Journal of Pure and Applied Chemistry Research 4 (1): 17–24. https://doi.org/10.21776/ub.jpacr.2015.004.01.203.

17. Hardeli, R. Zainul, dan L. P. Isara. 2019. "Preparation of Dye Sensitized Solar Cell (DSSC) using anthocyanin color dyes from jengkol shell (Pithecellobium lobatum Benth.) by the gallate acid copigmentation." Journal of Physics: Conference Series 1185 (1). https://doi.org/10.1088/1742-6596/1185/1/012021.

18. Shahzad, Nadia, D. Pugliese, A. Lamberti, A. Sacco, A. Virga, dan R. Gazia. 2013. "Monitoring the dye impregnation time of nanostructured photoanodes for dye sensitized solar cells." Journal of Physics: Conference Series 439 (1). https://doi.org/10.1088/1742-6596/439/1/012012.

19. Jena, Ajay K., dan Parag Bhargava. 2015. "Effect of amount of dye in the TiO2 photoanode on electron transport, recombination, Jsc and Voc of dye-sensitized solar cells." RSC Advances, no. 207890.

20. Cho, Seong Il, Hye Kyeong Sung, Sang Ju Lee, Wook Hyun Kim, Dae Hwan Kim, dan Yoon Soo Han. 2019. "Photovoltaic performance of dye-sensitized solar cells containing ZnO microrods." Nanomaterials 9 (12): 1–12. https://doi.org/10.3390/nano9121645.

21. Choi, Jongwan, dan Felix Sunjoo Kim. 2018. "Photoanode Thickness Optimization and Impedance Spectroscopic Analysis of Dye-Sensitized Solar Cells based on a Carbazole-Containing Ruthenium Dye." Journal of the Korean Physical Society 72 (5): 639–44. https://doi.org/10.3938/jkps.72.639.
22. Lim, Su Pei, Alagarsamy Pandikumar, Hong Ngee Lim, Ramasamy Ramaraj, dan Nay Ming Huang. 2015. "Boosting photovoltaic performance of dye-sensitized solar cells using silver nanoparticle-decorated N,S-Co-doped-TiO2 photoanode." Scientific Reports 5 (November 2014): 1–14. https://doi.org/10.1038/srep11922.
23. Mahbuburrahman, Md, Narayan Chandradebnath, dan Jae Joon Lee. 2015. "Electrochemical Impedance Spectroscopic Analysis of Sensitization-Based Solar Cells." Israel Journal of Chemistry 55 (9): 990–1001. https://doi.org/10.1002/ijch.201500007.
24. Zatirostami, Ahmad. 2020. "Increasing the efficiency of TiO2-based DSSC by means of a double layer RF-sputtered thin film blocking layer." Optik 207 (February). https://doi.org/10.1016/j.ijleo.2020.164419.